Experimental investigation of the flow inside a saxophone mouthpiece by particle image velocimetry

V. Lorenzoni[a)]
Aerodynamic Department, Siemens Wind Power, Dybendalsvaenget 3, 2630 Taastrup, Denmark

D. Ragni
Faculty of Aerospace Engineering–Aerodynamic Section, Delft University of Technology, Kluyverweg 2 2629 HT, Delft, The Netherlands

(Received 9 December 2010; revised 11 September 2011; accepted 15 September 2011)

An experimental study of the flow inside a saxophone mouthpiece in playing conditions is carried out by means of particle image velocimetry at high acquisition rate. Planar velocity measurements on the midsection of a Plexiglas tenor saxophone mouthpiece are performed, respectively, in the mouthpiece baffle and in the reed channel. Sequences of velocity fields inside the mouthpiece baffle and around the reed tip are shown for one reed duty cycle. Maxima of the velocity fluctuations are observed at the upper surface of the mouthpiece at a distance between five and ten reed apertures from the tip. The proper orthogonal decomposition analysis reveals that almost 50% of the kinetic energy in the baffle is distributed in the first two modes displaying a periodic behavior at the fundamental frequency, the rest being turbulent flow behavior. The measured dynamical vena contracta coefficient at the inlet is reasonably constant around the value of 0.6 for reed positions far from closure. This is in agreement with existing steady flow analytical models and previous experimental results. © *2012 Acoustical Society of America*. [DOI: 10.1121/1.3651795]

PACS number(s): 43.75.Pq [TRM] Pages: 715–721

I. THEORETICAL BACKGROUND AND INTRODUCTION

The operating principle of reed wind instruments (e.g., saxophones, clarinets, bassoons) is commonly described by the coupling of a linear passive resonator—the bore—and a nonlinear driving element represented by the reed–mouthpiece system.[1,2] The system operates in a closed feedback loop as a self-sustained oscillator in which the reed regulates the flow entering the mouthpiece and is in turn driven by the acoustic/hydrodynamic field.

Characteristics and properties of the linear resonator have been widely investigated both experimentally and theoretically,[3,4] also including the influence of side holes and wall vibrations.[5] The distribution of the pipe modes was shown to be a determinant coefficient for the musical quality of the instrument.

Contrarily, the nonlinear element has only recently been thoroughly investigated and the amount of experimental data is still limited. The work of Benade[3] revealed that the geometry of the mouthpiece baffle has a strong influence on the musical performances of the instruments, regarding both spectral distribution and emission facility, as also confirmed by the experience of manufacturers. The nonlinearity is represented by the relationship between the pressure difference across the reed Δp and the volume flow Φ at the inlet of the pipe. The first analytical relation based on experimental data fitting was proposed by Backus[6] for low blowing pressures as follows:

$$\Phi \propto \Delta p^{2/3} h^{4/3}, \tag{1}$$

where h indicates the reed aperture at the tip. Most models nowadays are based on the stationary Bernoulli relation in the assumption that for low playing frequencies (compared to the reed resonance frequencies) and reasonable blowing pressure (high Reynolds numbers, based on the reed aperture $\mathrm{Re} = \Phi/W\nu$) the flow in the reed channel can be considered to be frictionless, incompressible and quasi-stationary[7] as follows:

$$\Phi_B = hW\sqrt{\frac{2|\Delta p|}{\rho}}\mathrm{sgn}(\Delta p), \tag{2}$$

where W indicates the channel width, ρ the density of air, and ν the kinematic viscosity of air.

The presented model provided good agreement with experiments and has been adopted by many authors.[8] It however fails at explaining more complex behaviors in the presence of unsteady phenomena and for low Reynolds numbers (e.g., reed near closure).[7] A more complex model has been proposed by Hirschberg *et al.*,[9] based on the results of a steady flow simulation in a two-dimensional Borda tube. The model was further developed by van Zon *et al.*[10] and van Zon[11] who performed flow visualizations and laser doppler velocimetry (LDV) measurements on a two-dimensional model of the mouthpiece with fixed reed position. Two limit cases were found depending on the Reynolds

[a)]Author to whom correspondence should be addressed. Electronic mail: valerio.lorenzoni@siemens.com

number and ratio between the channel length L and the reed aperture h. For low Reynolds numbers [$\mathrm{Re}(h/L) << 1$] and long reed channels ($L/h > 10$) the flow was shown to be attached to the channel and well approximated by a fully developed two-dimensional Poiseuille flow:

$$\Phi = \frac{Wh\Delta p}{12\rho\nu L}, \tag{3}$$

which corresponds to the case of a reed almost closed. At high Reynolds numbers [$\mathrm{Re}\ (h/L) > 10$] and for short reed channels ($L/h < 2$) the flow separates at the sharp edge of the reed at the channel entrance and forms a jet of section S_j smaller than the opening cross section $S = Wh$. The volume flow was described by the following relation:

$$\Phi = \alpha Wh\sqrt{\frac{2|\Delta p|}{\rho}}\mathrm{sgn}(\Delta p), \tag{4}$$

where $\alpha = S_j/S = \Phi/\Phi_B$ is the so-called "vena contracta" coefficient. For two-dimensional mouthpiece geometries values in the range $0.5 < \alpha < 0.61$ are expected. This has been confirmed by the measurements of van Zon *et al.*[10] For intermediate flow conditions [$\mathrm{Re}(h/L) = O(1)$] and sufficiently long reed channels ($L/h > 4$), reattachment of the flow in the reed channel will occur after a distance of the order of $2h$ from the channel entrance due to momentum transfer by viscosity. The Bernoulli equation applies in the separated region and the flow approaches a Poiseuille flow after reattachment. The intermediate flow can be described by a boundary layer flow. The predicted flow behavior was in agreement with the measurements for Reynolds numbers below $\mathrm{Re} = 4000$, after which the flow becomes turbulent and the theory no longer applies. Such high Reynolds numbers are, however, not commonly reached in typical wind instruments, e.g., saxophones and clarinets.

The above model is based on a simplified two-dimensional geometry and assumes fixed separation point and uniform section of the reed channel, which might be questionable in the case of real mouthpieces, as already pointed out by Dalmont *et al.*[12] They performed experiments on a real clarinet mouthpiece to determine the reed opening by means of a laser inside the mouthpiece and a photoelectric diode, similarly to Backus.[13] The flow entering the mouthpiece was determined using a differential pressure meter across an orifice and the steady Bernoulli equation. The results qualitatively revealed that a constant vena contracta α, according to the findings of van Zon *et al.* is a reasonable first approximation for sufficiently large reed openings. The values of α measured by Dalmont *et al.*[12] on the real mouthpiece were however higher than for the simplified two-dimensional geometry of van Zon *et al.*[10]

Recently da Silva *et al.*[14] performed two-dimensional lattice-Boltzmann flow simulations on a model of a clarinet mouthpiece for different lay geometries without pipe. They found good agreement of the simulations with the steady experiments by van Zon *et al.*[10] and van Zon.[11] The agreement, however, degenerated during dynamic reed movements and the vena contracta coefficient was shown to be constant for only about 40% of the duty cycle. Due to the absence of the pipe, the oscillation frequency and the corresponding Strouhal number were an order of magnitude higher than under normal operating conditions. This could partially explain large deviations from a quasi-steady behavior. Further investigations were required in order to study the channel flow behavior at lower Strouhal numbers and three-dimensional effects.

This paper presents the results of velocity measurements conducted within a tenor saxophone mouthpiece in playing conditions using particle image velocimetry (PIV). These provide information on the flow patterns inside the mouthpiece and aim at validating some of the present models of reed channel flow. The analysis is performed on two different fields of view named, respectively, large field of view (LFOV) and zoomed field of view (ZFOV). An overview of the flow pattern inside the mouthpiece baffle is provided by the LFOV. The ZFOV provides visualization at higher spatial resolution of the flow at the mouthpiece inlet, which is used for evaluation of the vena contracta coefficient. The measured local vena contracta coefficient is compared with the predictions based on the model of Hirschberg *et al.*,[9] van Zon *et al.*,[10] and van Zon[11] and the results of da Silva *et al.*[14] and Dalmont *et al.*[12]

The paper is organized as follows: The experimental setup is described in Sec. II A. Section II B 1 shows the results of the PIV measurements inside the mouthpiece baffle including a proper orthogonal decomposition (POD) analysis. In Sec. II B 2 the flow measurements at the mouthpiece tip are presented together with the method for evaluation of the vena contracta coefficient.

II. EXPERIMENT

The flow inside a tenor saxophone mouthpiece is measured by particle image velocimetry (PIV). PIV is a nonintrusive experimental technique to measure the velocity of a fluid on a distributed region of space. The working principle can be briefly described as follows. Seeding particles are injected into the flow and illuminated by a laser. A couple of subsequent images of the illuminated particles are recorded by cameras and the particles' displacement between the two images is reconstructed by correlation techniques. This allows determining the velocity of the particles and, consequently, the flow velocity. For a detailed description of the technique the reader is referred to Raffel *et al.*[15]

A. Experimental setup

The whole experimental campaign is carried out in the High Speed Laboratories (HSL) of the Delft University of Technology. A transparent Plexiglas tenor saxophone mouthpiece by Hans Zinner GmbH & Co. KG® (Marktrodach, Germany) (M 7) (length 100 mm, internal baffle width $W = 15.6$ mm and tip aperture at rest $H = 1.9$ mm) is used in the present experiments. The internal edge of the mouthpiece is rounded, as it is commonly the case for commercial mouthpieces. Therefore, the length of the reed channel is not unequivocally defined. One external side of the baffle was lathed flat in order to avoid optical distortions when looking

through it. The same reed is used for all the tests. This is a commercially available Rico® (D'Addario & Co., Farmingdale, NY) wooden reed (measure 2) and it is covered by a black coating of paint in order to avoid light reflections.

The air is supplied by a storage vessel and premixed with seeding particles produced by a PIVTEC (Göttingen, Germany) PIVpart45 atomizer before entering the artificial mouth. The seeding particles consist of di-ethyl-hexyl-sebacat (DEHS) droplets of about 1 μm diameter with a relaxation time of 2 μs. A Plexiglas box of dimensions $130 \times 100 \times 100$ mm^3 and 6 mm thickness constitutes the artificial mouth, similar to the one used by Dalmont *et al.*[12] A rubber tube filled with water is used to simulate the player's lips. This tube is mounted on a flat metal support of 30 mm width and pressed against the reed ($\sim$1.5 cm from the tip) using two screws of a manually regulated height [see Fig. 1(a)].

Illumination inside the mouthpiece is provided by a double cavity Quantronix (East Setauket, NY) Nd-YLF laser, which produces an output of 2×12 mJ at 2 700 Hz. The laser sheet produced by a combination of optical lenses is focused on the mouthpiece midsection coming from upstream and has a thickness of $\sim$1 mm. The beam is inclined at 30° to the mouthpiece central line [see sketch of Fig. 1(a)] in order to minimize reflections of the light. Shadow regions due to light refraction through the mouthpiece edges are also minimized in this way. A complementary metal–oxide–semiconductor (CMOS) LaVision (Göttingen, Germany) HighSpeed camera is mounted above the box as shown in Fig. 1(b). This is equipped with a

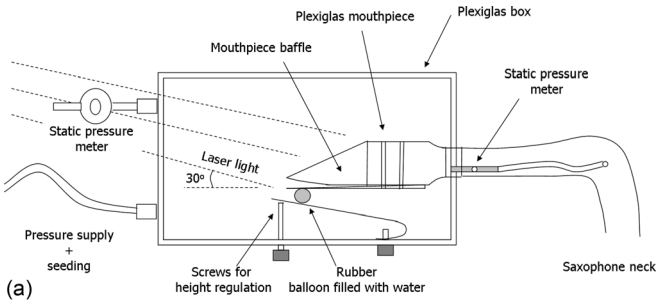

(a)

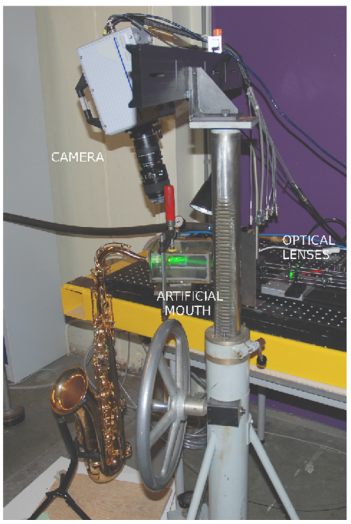

(b)

FIG. 1. (Color online) Schematic of the equipped artificial mouth (a) and overview of the complete setup (b).

Nikon® (Tokyo, Japan) objective of 105 mm focal length and a 100 mm optical extension with Scheimpflug adaptor. The numerical aperture is set to $f\# = 5.6$. Synchronization between laser and cameras is performed by means of a LaVision high-speed controller and the acquisition is controlled by a PC with the DAVIS 7.4 software by LaVision.

A commercial tenor saxophone Winston Boston® (Charleston, SC) is directly connected to the mouthpiece as shown in Fig. 1(b). The mouthpiece is rotated 90° sideward with respect to the normal playing position. This was shown to neither influence the flow behavior nor the sound production. During the experiments the air supply is adjusted in order to produce a B3 note (in equal temperament system), which corresponds to a frequency $f = 247$ Hz. The static pressure difference across the reed Δp is recorded by a digital pressure gauge by Mensor® (San Marcos, TX) connected to two static ports, placed, respectively, on the internal sidewall of the box and in the aft part of the mouthpiece as indicated in the sketch of Fig. 1. The latter is constituted by a metal cylinder of diameter $D_p = 2$ mm and length $L_p = 40$ mm aligned with the flow with a side hole at $\sim 15 D_p$ from the tip. The presence of the probe was shown to have neither influence on the flow features inside the mouthpiece, nor on the sound production.

B. Results

Planar PIV measurements at the midspan section of the mouthpiece are carried out on two different fields of view: large field of view (LFOV) embracing the whole mouthpiece baffle and a zoomed field of view (ZFOV) focused on the reed–mouthpiece tip. The former allows for the visualization of the characteristics of the turbulent flow inside the mouthpiece, whereas the latter provides a visualization of the reed channel flow, which is useful for the comparison with the flow models discussed in Sec. I. Before the acquisition, the position of the artificial lips and the differential pressure are manually adjusted until the saxophone produces a stable note. Typical differential pressure used is $\Delta p \sim 30$ mbar.

The PIV system is operated at 2700 Hz yielding a temporal resolution of 370 μs, which corresponds to $\sim$11 velocity fields per reed opening/closing cycle. The total duration of an acquisition is 1 s, thus providing ensembles of 2700 samples per run. The velocity field from the PIV recordings is evaluated using the multipass window deformation cross-correlation algorithm developed by Scarano and Riethmuller[16] and implemented in the LaVision DAVIS 7.4 software package. The bias error caused by peak locking is minimized by ensuring a particle image diameter of $\sim$2 pixels.[15] Flow motion perpendicular to the measuring plane is not taken into account by the present measurement.

1. Large field of view

The LFOV is a square of dimensions 25.9×25.9 mm^2 and allows for measuring the velocity field inside the mouthpiece baffle. The use of a final correlation window of size 12×12 pixels with 50% overlap provides a space resolution of 0.2 mm/vector. A time sequence of contours of velocity magnitude ($V = \sqrt{u^2 + v^2}$) during one reed opening/closing cycle is shown in Fig. 2. The significant snapshots have been

chosen for the visualization. The direction of motion is indicated by the vectors and the raw image is kept as background, in order for the reader to easily recognize the position of the reed. The origin of the reference frame has been chosen to coincide with the tip of the mouthpiece. The nondimensional time t^* is obtained by normalizing the physical time t (in seconds) by the oscillation period $T = 1/f_m$, where f_m is the oscillation frequency in measuring conditions ($f_m = 237$ Hz from POD analysis, see later in this section). The images are corrected for warping due to the inclination of the objective plane with the measuring plane (about 10°).

The flow direction is from left to right. The velocity magnitude features maxima of over 60 m/s and the region of highest velocity is mainly concentrated along the upper surface of the mouthpiece, as also observed in the velocity fields of da Silva *et al.*[14] for short channel geometry. The reed starts opening from $t^* = 0$ to $t^* = 0.18$. Inversion of motion is then observed between $t^* = 0.26$ and $t^* = 0.35$ (not shown), which corresponds to a local increase of the velocity downstream of the reed channel. Successively, the reed opens again between $t^* = 0.44$ and $t^* = 0.54$ (not shown) with a lower displacement than the initial one. When the reed starts closing there is a sudden acceleration of the flow just after the reed channel and a jet of high velocity is formed in the middle of the mouthpiece ($t^* = 0.61$). The high velocity region is displaced toward the upper surface of the mouthpiece ($t^* = 0.7$). After $t^* = 0.7$ the reed approaches closure and remains almost closed for the rest of the duty cycle. The same nonsinusoidal motion of the reed is observed for all the runs when the mouthpiece is connected to the bore. The presence of a nonzero velocity region around $x = 5H$ (where H indicates the reed aperture at rest) after closure of the reed (e.g., $t^* = 0$) is ascribed to transversal movements of the reed and three-dimensional flow recirculation inside the mouthpiece. At large reed apertures the direction of the flow motion is rather uniform in the central part of the mouthpiece (around $y = 0$) and vortical structures (indicated by the rotational pattern of the vectors) are mainly concentrated downstream (toward the mouthpiece chamber).

The mouthpiece surface in Fig. 3 is colored gray. The reed is black and placed in an intermediate position, whereas the area swept by the reed is colored white. Figure 3(a) shows contours of the mean velocity magnitude calculated over 2700 velocity fields. These feature maxima of ~40 m/s localized on the upper surface between $x = 5H$ and $10H$ and less than 50% at the exit of the reed channel. The high velocity in the same region is also observed in the sequence of Fig. 2 and explains why the internal geometry of the mouthpiece baffle is known to have such a strong influence on the sound production, as reported by Hirschberg *et al.*[7] and also experienced by the authors.

Contours of the root mean square of the velocity fluctuations are shown in Fig. 3(b). These reveal that the largest fluctuations have an intensity of over 50% normalized with the local mean velocity and are concentrated around $x = 8\,H$ downstream from the channel entrance, where the breakup of the jet produced at the reed channel occurs. These fluctuations are due both to the periodic motion induced by the reed oscillations and to the superimposed turbulence fluctuations. The velocity field is decomposed by POD.[17] This method is based on the projection of the fluctuating part of the velocity field onto a set of orthogonal basis and allows separating highly energetic large structures from the smaller turbulent fluctuations. The analysis reveals that the first two POD modes contain the largest percentage of the total kinetic energy (respectively, 35% mode 1 and 12% mode 2). The modal decomposition allows the evaluation of the spectral content of the fluctuating velocity field.

The spectra are normalized with the total energy of the mode in all the snapshots. Figure 4 indicates that the motion has a strong tonal peak for the first two POD modes at 237 Hz. This frequency is ~4% lower than the nominal playing frequency. Indeed during the acquisitions, an audible pitch decrease of the note played by the saxophone is noticed when the mouthpiece is illuminated by the laser light. This is

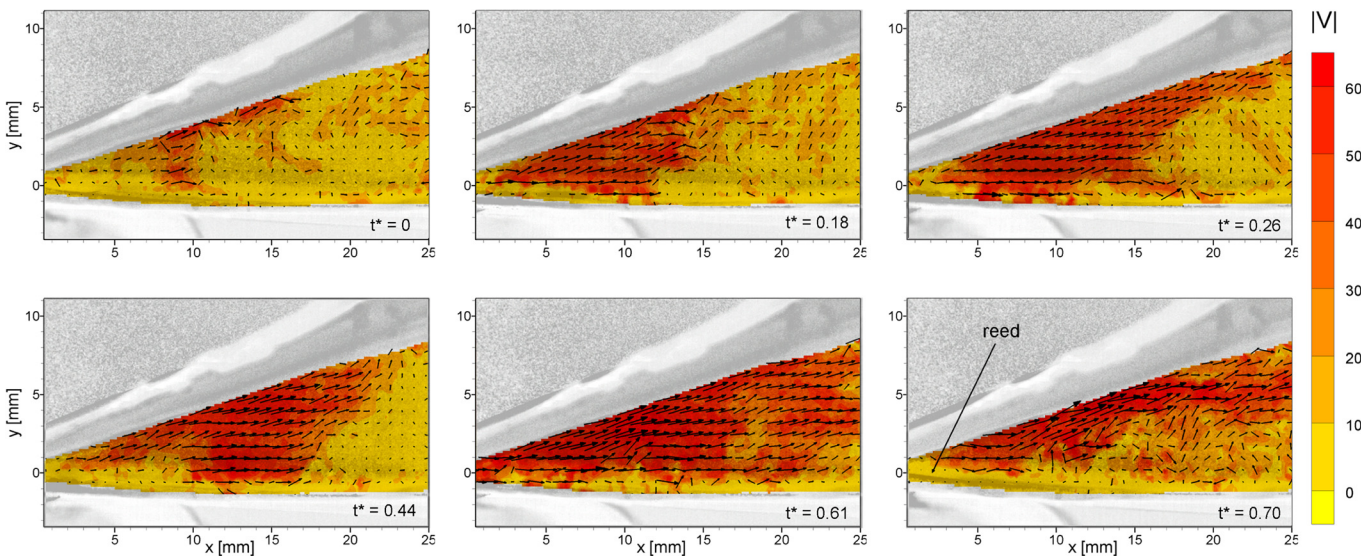

FIG. 2. (Color online) Sequence of contours and vectors of velocity magnitude inside the mouthpiece during one duty cycle. Raw image from the acquisition in background. Vectors displayed every three points in the x and y direction.

ascribed to the warming up of the reed with consequent change of its elastic properties. Higher modes feature no tonal components and are associated with turbulent fluctuations. It can be concluded that ~53% of the kinetic energy of the flow inside the baffle is associated with turbulent fluctuations.

2. Zoomed field of view

Visualization of the reed channel flow is made by using a ZFOV of dimensions 13.8×13.8 mm^2 around the reed–mouthpiece tip. A window size of 8×8 pixels with 50% overlap allows for a space resolution of 0.056 mm/vector. The average pressure difference across the reed in this case corresponds to 28.6 mbar (reference Bernoulli velocity $U_B = \sqrt{2|\Delta p|/\rho} = 68.3$ m/s).

The areas where velocity measurements are not reliable, are painted white for clarity. Analogous to the behavior observed in the sequence of Fig. 2, the reed opens in the first part of the cycle, starts closing again after $t^* = 0.18$, reopens with lower displacement until $t^* = 0.61$ and approaches closure after $t^* = 0.7$. After $t^* = 0.7$ there is no optical access to the reed channel and velocity measurements cannot be performed.

The flow undergoes a strong acceleration in the first phase of the cycle with maximum velocity of over 70 m/s between h and $2h$ downstream of the reed tip (where h indicates the instantaneous reed aperture) in agreement with the LDV measurements of van Zon on a fixed two-dimensional channel (see Fig. 2.21 in van Zon[11]). The velocity field presents a higher level of uniformity compared to the visualizations of Fig. 2 and the flow is believed to be dominantly two-dimensional in the reed channel. The uniformity decreases for large reed apertures and at large distances from the tip ($x > 2h$–$3h$), where recirculation occurs. The detachment–reattachment phenomenon described by van Zon *et al.* and da Silva *et al.* is not observed at the present space resolution.

The volume flux through the mouthpiece inlet Φ is calculated on the control surface Γ at the reed tip $x = 0.6$ mm (indicated in Fig. 5 at time instant $t^* = 0.44$), in the assumption of two-dimensional flow along the reed channel width. This assumption is justified by the previous results and the large aspect ratio $W/h > 7$ in playing conditions. At the low Mach number of the present experiment (Ma < 0.2) the flow is considered incompressible. The mean volume flux through the mouthpiece is $\bar{\Phi} = 3.8 \times 10^{-4}$ m^3/s.

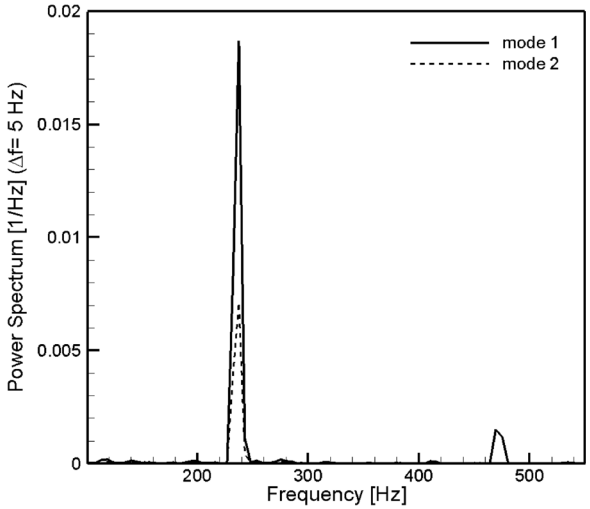

FIG. 4. Power spectrum of the first and second POD modes.

The vena contracta coefficient, α, of Eq. (4) is calculated as the ratio between the average velocity at the inlet $v_{av} = \Phi/hw$ and the maximum velocity in the reed channel downstream of the reed tip between $x = h$ and $x = 2h$, where the velocity was shown to feature a local maximum.

The data points in Fig. 6 correspond to the eight images shown in Fig. 5 and each point is obtained by averaging over 50 duty cycles. The values of α between $t^* = 0.09$ and $t^* = 0.7$ are reasonably constant around 0.6 with standard deviations about the mean σ_α (indicated by the error bars) below 10%. The highest standard deviations are observed at $t^* = 0.09$ ($\sigma_\alpha = 30\%$) and $t^* = 0.7$ ($\sigma_\alpha = 50\%$) and correspond to the phases when the reed is near closure. The large variations of α near closure are due to scarce optical accessibility to the channel flow.

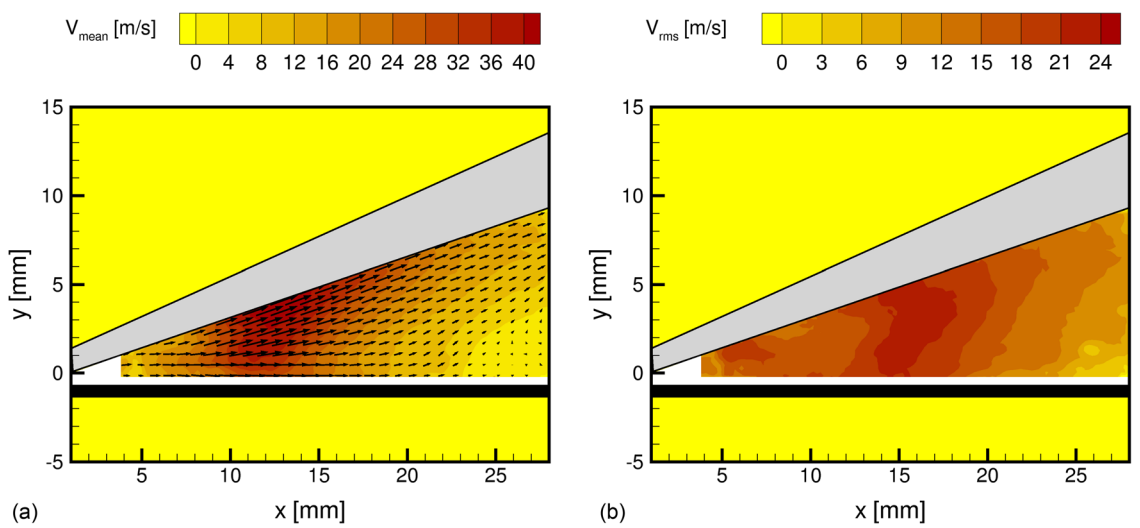

FIG. 3. (Color online) (a) Mean velocity magnitude and (b) root mean square of the velocity fluctuations.

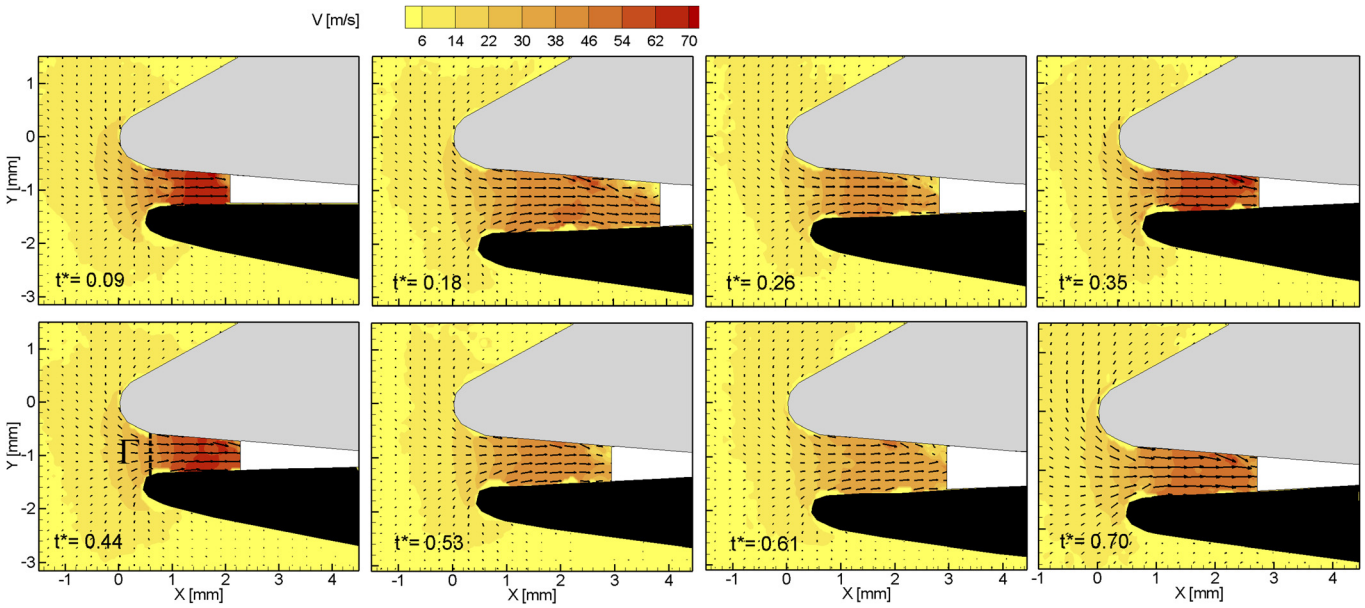

FIG. 5. (Color online) Sequence of contours and vectors of velocity magnitude around the mouthpiece tip during one duty cycle. Vectors displayed every five points in the x direction and three points in the y direction. Control surface Γ for evaluation of the volume flux and reed aperture ($t^* = 0.44$).

The results are in good agreement with the quasi-stationary model proposed by Hirschberg *et al.*[9] and van Zon *et al.*,[10] which predicts a constant vena contracta between 0.5 and 0.61, indicated by the dashed line. Similar results were obtained by van Zon[11] using experimental velocity data on an oscillating valve for low Strouhal numbers and in the simulations of da Silva *et al.*[14] for the short reed channel geometry. In the latter case scattering of the values was observed near reed closure and was ascribed to the higher contribution of the flow driven by the reed with respect to the pressure driven flow. The present analysis cannot confirm such a conclusion as no PIV measurements can be performed when the reed is approaching closure due to scarce optical accessibility. Experimental results on a clarinet mouthpiece by Meynial *et al.*[18] report a value of α between 0.6 and 0.85. Dalmont *et al.*[12] found a constant value of $\alpha \sim 0.95$ for a large part of the duty cycle. In the latter analysis the flux from the lateral sides of the reed channel is included. This can explain the higher values of α compared to the present observations, which concern the flow on a plane at the symmetry axis of the reed.

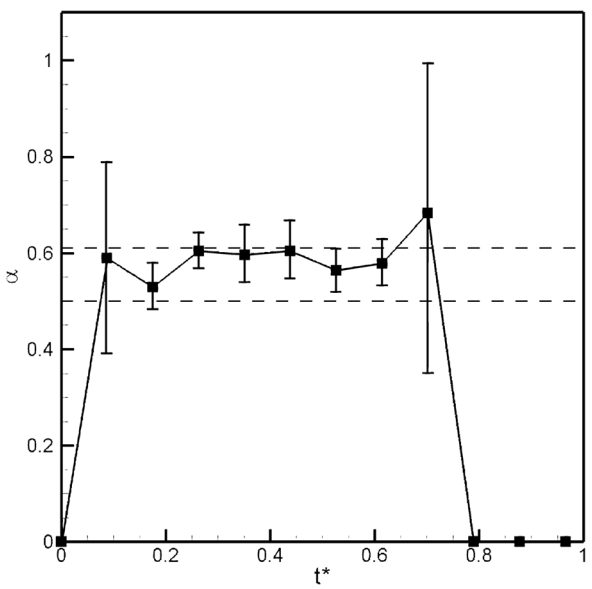

FIG. 6. Vena contracta coefficient, α, during one duty cycle with error bars (solid line), theoretical limits for two-dimensional Borda tube (dashed lines).

III. CONCLUSIONS

An experimental investigation of the flow inside a tenor saxophone mouthpiece was carried out by particle image velocimetry at high acquisition rate. Two different fields of view were analyzed: A large field of view (LFOV) embracing the mouthpiece baffle and a zoomed view around the reed–mouthpiece tip (ZFOV).

The former analysis revealed that the mean velocity in the baffle features maxima in proximity of the upper surface between $5H$ and $10H$ downstream of the inlet. The internal geometry of such part is therefore considered having an important influence on the sound production as also reported by Hirschberg *et al.*[7] Velocity fluctuations inside the mouthpiece baffle reach maxima of 55% the local mean velocity. The highest values appear in correspondence of the breakup of the jet where three-dimensional motion is likely to occur. From the POD analysis it was observed that ~47% of the kinetic energy of the flow fluctuations around the mean, is distributed in the first two modes at the fundamental reed oscillation frequency, whereas ~53% is distributed into turbulent motion.

The measurements on the ZFOV showed that the flow in the first part of the mouthpiece inlet is dominantly two dimensional. Velocity maxima of ~70 m/s were observed between $1h$ and $2h$ downstream from the reed tip, when the

reed is almost closed. The vena contracta coefficient α during one duty cycle was calculated as the ratio between volume flux at the reed tip and the maximum velocity at a distance between one and two reed apertures downstream of the tip. For large reed openings, the values of α were found to be rather constant around the value 0.6, with the largest standard deviations near reed closure.

The results are in good agreement with the flow model of Hirschberg *et al.*[9] and van Zon for short reed channels and with the experimental results of van Zon[11] for an oscillating valve at low Strouhal numbers. A constant vena contracta of $\sim$0.6 for $\sim$40% of the duty cycle also resulted from the two-dimensional numerical simulations of da Silva *et al.*[14] From the present analysis it can be concluded that a quasi-stationary Bernoulli model with a constant vena contracta of 0.6 is a valid approximation for single reeds woodwind instrument for sufficiently large reed apertures.

Future work is needed in order to take into account three-dimensional flow motion. The use of a specifically designed mouthpiece with a squared internal baffle chamber is also required to increase optical accessibility to the flow. The work of Ducasse[19] has shown that sound synthesis of single-reed musical instruments can be obtained by the use of simplified models based on their functioning principle. Validation of such models through experimental analysis is an important step toward further developments of computer music and manufactural improvements.

ACKNOWLEDGMENTS

The authors would like to thank Professor F. Scarano for the use of the experimental facilities and the helpful suggestions. Special thanks are given to Dr. C. J. Nederveen for the valuable directions on the design of the experimental setup. Professor A. (Mico) Hirschberg and Dr. A. da Silva are also gratefully acknowledged for the insightful comments and discussions during the elaboration of the paper.

[1]M. E. McIntyre, R. T. Schumacher, and J. Woodhouse, "On the oscillation of musical instruments," Exp. Fluids **74**, 1325–1345 (1983).

[2]A. Hirschberg, X. Pelorson, and J. Gilbert, "Aeroacoustics of musical instruments," in *Meccanica* (Springer, New York, 1996), Vol. 31, No. 2, pp. 131–141.

[3]A. H. Benade, *Fundamentals of Musical Acoustics* (Oxford University Press, Oxford, UK, 1976), Chaps. 21 and 22.

[4]N. H. Fletcher, "Air flow and sound generation in musical wind instruments," Annu. Rev. Fluid Mech. **11**, 123–146 (1979).

[5]C. J. Nederveen and J. P. Dalmont, "Pitch and level changes in organ pipes due to wall resonances," J. Acoust. Soc. Am. **271**, 227–239 (2004).

[6]J. Backus, "Small vibration theory of the clarinet," Exp. Fluids **26**, 513–523 (1963).

[7]A. Hirschberg, J. Gilbert, A. P. J. Wijnands, and A. M. C. Valkering, "Musical aero-acoustics of the clarinet," J. Phys. (Paris), Colloq. **4**, 559–568 (1994).

[8]N. H. Fletcher and T. D. Rossing, *The Physics of Musical Instruments* (Springer, New York, 1998), Chap. 13.

[9]A. Hirschberg, W. A. van de Laar, J. P. Marrou-Maurieres, P. J. Wijnands, H. J. Dane, S. G. Kruijswijk, and A. J. M. Houtsma, "A quasi-stationary model of air flow in the reed channel of single reed woodwind instruments," Acoustica **70**, 146–154 (1990).

[10]J. C. P. van Zon, A. Hirschberg, J. Gilbert, and A. P. J. Wijnands, "Flow through the reed channel of a single reed music instrument," J. Phys. (Paris), Colloq. **51**, 821–824 (1990).

[11]J. C. P. van Zon, "Stromingsgeïnduceerde klepinstabiliteiten (Flow-induced valve instabilities)," M.Sc. thesis, Technical University of Eindhoven, Eindhoven, The Netherlands, 1989.

[12]J. P. Dalmont, J. Gilbert, and S. Ollivier, "Nonlinear characteristics of single-reed instruments: quasistatic volume flow and reed opening measurements," J. Acoust. Soc. Am. **114**, 2253–2261 (2007).

[13]J. Backus, "Vibrations of the reed and the air column in the clarinet," J. Acoust. Soc. Am. **33**, 806–809 (1961).

[14]A. R. da Silva, G. P. Scavone, and M. van Wallstijn, "Numerical simulations of fluid-structure interactions in single-reed mouthpieces," J. Acoust. Soc. Am. **122**, 1798–1808 (2007).

[15]M. Raffel, C. Willert, and J. Kompenhans, *Particle Image Velocimetry: A Practical Guide* (Springer, Berlin, 2007), Chaps. 1–6.

[16]F. Scarano and M. L. Riethmuller, "Advances in iterative multigrid PIV image processing," Exp. Fluids **29**, 51–60 (2004).

[17]L. Cordier and M. Bergmann, "Proper orthogonal decomposition: An overview," *Post-Processing of Numerical and Experimental Data* (von Karman Institute, Rhode-St-Genèse, Belgium, 2008), Chap. 5, LS 2008-01.

[18]X. Meynial, J. Gilbert, and A. Hirschberg, "Étude expérimentale des grandeurs d'entrée d'un résonateur de forme simple couplé a une anche simple (Experimental study of the inlet quantities of a simple-shaped resonator coupled to a simple reed)," J. Phys. (Paris), Colloq. **2**, 75–78 (1992).

[19]E. Ducasse, "Modélisation d'instruments de musique pour la synthèse sonore: Application aux instruments à vent (Modeling of musical instruments for sound synthesis: Application to wind instruments)," J. Phys. (Paris), Colloq. **51**, 837–840 (1990).